FREQUENCY OFFSET ESTIMATION FOR GALILEO/GPS RECEIVERS BASED ON DIFFERENTIAL CORRELATION

Andreas Schmid and André Neubauer

Infineon Technologies AG
Development Center NRW

Christoph Günther

Technical University Munich, and
German Aerospace Center

ABSTRACT

Urban and moderate indoor applications of Galileo/GPS receivers require particularly high reception sensitivity. Residual frequency deviations due to unknown Doppler frequency shifts degrade the reception sensitivity. Estimation of the frequency offset can therefore substantially enhance the reception sensitivity of Galileo/GPS receivers. This paper presents a frequency estimation method that is especially tailored for Galileo/GPS receivers using differential correlation. It is suitable for the very low signal to noise ratios of attenuated Galileo/GPS signals and introduces very little additional implementation complexity. The performance analysis presented in this paper shows promising results for an application in next generation Galileo/GPS receivers.

1. INTRODUCTION

GPS and Galileo receivers have to perform CDMA acquisition with unknown Doppler frequency shifts in the range of $\pm 5\,\mathrm{kHz}$. The search space is therefore usually partitioned into search bins with the size inversely proportional to the coherent integration time. Only the center frequency of each search bin is then used for downconversion and the acquisition test. The remaining residual frequency deviation leads to a sensitivity degradation of the Galileo/GPS receiver. However, the Galileo/GPS signals can be received on earth surface with just $-158\,\mathrm{dBW}$ for line-of-sight propagation. The reception sensitivity is therefore one of the most important parameters for urban and moderate indoor environments. Estimating and correcting the residual frequency deviation can substantially improve reception sensitivity. It can further reduce the implementation complexity by decreasing the required number of frequency search bins.

There are many different methods for estimating a frequency offset [1] [2]. Many are optimized for special signal specifications or particular application domains [3] [4]. This paper presents a frequency estimation method that is of special practical relevance for Galileo/GPS receivers using differential correlation. It is tailored for the very low signal to noise ratios of Galileo/GPS signals and it introduces very little additional implementation complexity.

Section 2 discusses the Galileo/GPS receiver chain with its signal processing steps that are continued in section 3 with differential correlation. Section 4 introduces the frequency offset estimation algorithm, section 5 derives the probability density function of the estimated frequency deviation, and section 6 evaluates the presented method.

2. COHERENT PREDETECTION

In this section, the statistical properties of the coherent predetection result s_μ of the receiver channel in Fig. 1 will be derived. The received Galileo/GPS signal can be expressed in its complex-valued, low-pass equivalent, and sampled form as

$$r_\nu = \sqrt{2C} c_\nu \mathrm{e}^{\mathrm{j}(2\pi f_\mathrm{d} \nu T_\mathrm{s} + \phi)} + n_\nu, \qquad (1)$$

where C denotes the carrier power, c_ν the spreading code, f_d the residual frequency deviation, T_s the sample period, ϕ the unknown initial phase, and n_ν complex-valued, zero-mean, white Gaussian noise with variance

$$\sigma_n^2 = 2\mathrm{E}\left\{\Re\{n\}^2\right\} = 2\mathrm{E}\left\{\Im\{n\}^2\right\} = 2N_0BF. \qquad (2)$$

For simplicity of presentation, the data modulation of the Galileo/GPS signals is neglected in (1), since the data stream can be supplied by assistance data and is not even present in some of the Galileo signals. N_0 denotes the thermal noise power spectral density, F the receiver noise figure, and $B = 1/T_\mathrm{s}$ the filter bandwidth. The result after despreading and coherent integration

$$s_\mu = \sum_{\nu=\mu N}^{(\mu+1)N-1} r_\nu c^*_{\nu+\tau \bmod N} = a_\mu + w_\mu, \qquad (3)$$

can be approximated for sufficiently small frequency deviations by [5]

$$a_\mu \approx \sqrt{2C} R_\mathrm{c}(\tau) \mathrm{sinc}(f_\mathrm{d} T_\mathrm{i}) \mathrm{e}^{\mathrm{j}(\pi f_\mathrm{d}(2\mu+1)T_\mathrm{i} + \phi)}, \qquad (4)$$

where

$$R_\mathrm{c}(\tau) = \sum_{\nu=0}^{N-1} c_\nu c^*_{\nu+\tau \bmod N} \qquad (5)$$

0-7803-9404-6/05/$20.00 ©2005 IEEE

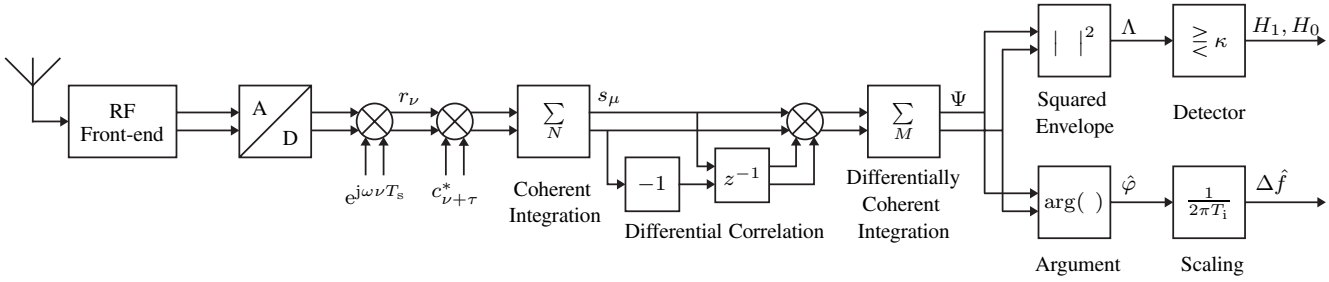

Fig. 1. Galileo/GPS receiver channel including the frequency offset estimation. The block diagram shows which signal processing steps can be reused from a receiver using differential correlation, as presented in the upper path of the diagram. The frequency estimation method is presented in the lower path of the diagram.

denotes the circular autocorrelation function of c_ν.

$$T_\mathrm{i} = NT_\mathrm{s} \tag{6}$$

is the coherent integration time, and w_μ complex-valued, zero-mean, white Gaussian noise with variance

$$\sigma_w^2 = 2\mathrm{E}\left\{\Re\{w\}^2\right\} = 2\mathrm{E}\left\{\Im\{w\}^2\right\} = 2N_0\frac{N^2}{T_\mathrm{i}}F. \tag{7}$$

3. DIFFERENTIAL CORRELATION RESULT

In [6], the statistical properties of the variable

$$\Psi = \sum_{\mu=1}^{M} s_\mu s^*_{\mu-1} \tag{8}$$

as pictured in Fig. 1 were derived in detail. Using the central limit theorem, it has been shown that the result after differential correlation converges very fast to a Gaussian-distributed variable with mean

$$\mathrm{E}\{\Psi\} = 2CR_c^2(\tau)\sum_{\mu=1}^{M}\Big[\mathrm{sinc}\left(f_{\mathrm{d},\mu}T_\mathrm{i}\right)\mathrm{sinc}\left(f_{\mathrm{d},\mu-1}T_\mathrm{i}\right) \cdot e^{j[\pi(f_{\mathrm{d},\mu}-f_{\mathrm{d},\mu-1})T_\mathrm{i}+\varphi_\mu-\varphi_{\mu-1}]}\Big] \tag{9}$$

$$\varphi_\mu = \varphi_{\mu-1} + 2\pi f_{\mathrm{d},\mu-1}T_\mathrm{i} \tag{10}$$

and variances

$$\mathrm{E}\left\{\left(\Re\{\Psi-\mathrm{E}\{\Psi\}\}\right)^2\right\} = M\frac{\sigma_w^4}{2}+\frac{\sigma_w^2}{2}\sum_{\mu=0}^{M}|a_{\mu+1}+a_{\mu-1}|^2 \tag{11}$$

$$\mathrm{E}\left\{\left(\Im\{\Psi-\mathrm{E}\{\Psi\}\}\right)^2\right\} = M\frac{\sigma_w^4}{2}+\frac{\sigma_w^2}{2}\sum_{\mu=0}^{M}|a_{\mu+1}-a_{\mu-1}|^2 \tag{12}$$

$$a_{-1} = a_{M+1} = 0. \tag{13}$$

It has be shown in [6] that this differential correlation method provides a sensitivity gain over conventional noncoherent integration of around 1.5 dB. Fig. 2 compares the actual result after differential correlation versus the corresponding Gaussian approximation. It can be seen that even for a very small $M = 4$, there is almost no observable difference. Real Galileo/GPS applications use a much larger noncoherent integration number M, often in the range of 50 to 1000. Inserting the constant frequency deviation f_d into (9), (11), and (12) yields

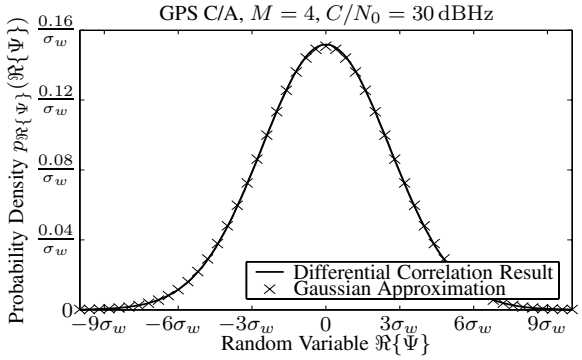

Fig. 2. Comparison of the differential correlation result $p_{\Re\{\Psi\}}(\Re\{\Psi\})$ versus the corresponding Gaussian approximation for a very small $M = 4$.

$$x \triangleq \Re\{\Psi\}, \quad y \triangleq \Im\{\Psi\} \tag{14}$$

$$m_x = \mathrm{E}\{x\} = M2CR_\mathrm{c}^2(\tau)\mathrm{sinc}^2(f_\mathrm{d}T_\mathrm{i})\cos(2\pi f_\mathrm{d}T_\mathrm{i}) \tag{15}$$

$$m_y = \mathrm{E}\{y\} = M2CR_\mathrm{c}^2(\tau)\mathrm{sinc}^2(f_\mathrm{d}T_\mathrm{i})\sin(2\pi f_\mathrm{d}T_\mathrm{i}) \tag{16}$$

$$\sigma_x^2 = \mathrm{E}\left\{(x-m_x)^2\right\} = M\frac{\sigma_w^4}{2} + 2CR_\mathrm{c}^2(\tau)\mathrm{sinc}^2(f_\mathrm{d}T_\mathrm{i})\sigma_w^2 \cdot \left[1+2(M-1)\cos^2(2\pi f_\mathrm{d}T_\mathrm{i})\right] \tag{17}$$

$$\sigma_y^2 = \mathrm{E}\left\{(y-m_y)^2\right\} = M\frac{\sigma_w^4}{2} + 2CR_\mathrm{c}^2(\tau)\mathrm{sinc}^2(f_\mathrm{d}T_\mathrm{i})\sigma_w^2 \cdot \left[1+2(M-1)\sin^2(2\pi f_\mathrm{d}T_\mathrm{i})\right] \tag{18}$$

4. ESTIMATION OF THE FREQUENCY OFFSET

As can be seen from (15) and (16), the phase of the expectation value of Ψ is proportional to the residual frequency deviation f_d

$$\mathrm{E}\{\Psi\} = M2CR_\mathrm{c}^2(\tau)\mathrm{sinc}^2(f_\mathrm{d}T_\mathrm{i})\mathrm{e}^{\mathrm{j}2\pi f_\mathrm{d}T_\mathrm{i}}, \tag{19}$$

$$\arg\left(\mathrm{E}\{\Psi\}\right) = 2\pi f_\mathrm{d}T_\mathrm{i}. \tag{20}$$

The residual frequency deviation f_d can therefore be estimated by

$$\hat{f}_\mathrm{d} = \frac{\arg(\Psi)}{2\pi T_\mathrm{i}} = \frac{\arg\left(\sum_{\mu=1}^{M} s_\mu s_{\mu-1}^*\right)}{2\pi T_\mathrm{i}}. \tag{21}$$

This estimate becomes more accurate the higher the signal-to-noise ratio of s_μ is and the larger M is. The signal to noise ratio of Ψ

$$\frac{\mathrm{E}\{|\Psi|\}^2}{\mathrm{E}\{|\Psi - \mathrm{E}\{\Psi\}|^2\}} = M\frac{|a|^4}{\sigma_w^4 + 2\sigma_w^2|a|^2} \tag{22}$$

increases proportional to M and the results of section 6 confirm that the standard deviation of the estimated frequency offset decreases significantly with increasing M.

The method in (21) applies the argument function only after the differentially coherent integration. It therefore solves the problem of phase jumps that occur when the imaginary part of the individual differential correlation results $s_\mu s_{\mu-1}^*$ introduce sign changes due to the added noise. Since the signal-to-noise ratios for indoor and urban GPS reception are often very low, such sign changes would occur frequently and result in a bias towards zero. Furthermore, applying the argument function after the differentially coherent integration allows the reuse of the existing averaging functionality that is already required for differential correlation.

As it can be seen in Fig. 1, the method in (21) can reuse most of the signal processing steps that are already present in receivers based on differential correlation and the only additionally required steps are calculating the phase of the differential correlation result and scaling it.

5. PROBABILITY DISTRIBUTION OF THE ESTIMATED FREQUENCY DEVIATION

This section derives the probability density function for the estimated frequency deviation $\hat{f}_\mathrm{d}$ according to (21). The complex Gaussian probability density of Ψ transformed into polar coordinates is

$$p_\Psi(r,\varphi) = \frac{r}{2\pi\sigma_x\sigma_y}\mathrm{e}^{\left(-\frac{(r\cos(\varphi)-m_x)^2}{2\sigma_x^2} - \frac{(r\sin(\varphi)-m_y)^2}{2\sigma_y^2}\right)}, \tag{23}$$

$$r = |\Psi|, \quad \varphi = \arg(\Psi), \quad \varphi \in [-\pi, \pi]. \tag{24}$$

With the substitutions

$$\alpha(\varphi) \triangleq \sqrt{\frac{\cos^2(\varphi)}{2\sigma_x^2} + \frac{\sin^2(\varphi)}{2\sigma_y^2}}, \tag{25}$$

$$\beta(\varphi) \triangleq \frac{m_x\cos(\varphi)}{\sigma_x^2} + \frac{m_y\sin(\varphi)}{\sigma_y^2}, \tag{26}$$

$$\gamma \triangleq \frac{\mathrm{e}^{\left(-\frac{m_x^2}{2\sigma_x^2} - \frac{m_y^2}{2\sigma_y^2}\right)}}{2\pi\sigma_x\sigma_y}, \tag{27}$$

(23) can be integrated over r to obtain the probability density of φ

$$p_\varphi(\varphi) = \gamma\int_0^\infty \mathrm{e}^{-\alpha^2(\varphi)r^2+\beta(\varphi)r}\, r\, dr. \tag{28}$$

The integral in (28) can be solved by quadratic extension

$$r \triangleq \frac{\rho}{\alpha(\varphi)} + \frac{\beta(\varphi)}{2\alpha^2(\varphi)}, \quad dr \triangleq \frac{1}{\alpha(\varphi)}\, d\rho, \tag{29}$$

$$\begin{aligned}
p_\varphi(\varphi) &= \frac{\gamma}{\alpha(\varphi)}\int_{-\frac{\beta(\phi)}{2\alpha(\varphi)}}^\infty \left(\frac{\rho}{\alpha(\varphi)} + \frac{\beta(\varphi)}{2\alpha^2(\varphi)}\right) \\
&\quad \cdot \mathrm{e}^{-\left(\rho+\frac{\beta(\varphi)}{2\alpha(\varphi)}\right)^2+\left(\frac{\beta(\varphi)\rho}{\alpha(\varphi)}+\frac{\beta^2(\varphi)}{2\alpha^2(\varphi)}\right)}\, d\rho \\
&= \frac{\gamma}{\alpha^2(\varphi)}\mathrm{e}^{\frac{\beta^2(\varphi)}{4\alpha^2(\varphi)}}\left[\int_{-\frac{\beta(\varphi)}{2\alpha(\varphi)}}^\infty \frac{\beta(\varphi)}{2\alpha(\varphi)}\mathrm{e}^{-\rho^2}\, d\rho\right. \\
&\quad \left. + \int_{-\frac{\beta(\varphi)}{2\alpha(\varphi)}}^\infty \mathrm{e}^{-\rho^2}\rho\, d\rho\right] \\
&= \frac{\gamma}{\alpha^2(\varphi)}\mathrm{e}^{\frac{\beta^2(\varphi)}{4\alpha^2(\varphi)}} \\
&\quad \cdot \left[\frac{\beta(\varphi)\sqrt{\pi}}{4\alpha(\varphi)}\mathrm{erf}(\rho) - \frac{1}{2}\mathrm{e}^{-\rho^2}\right]\Bigg|_{-\frac{\beta(\varphi)}{2\alpha(\varphi)}}^\infty,
\end{aligned} \tag{30}$$

resulting in

$$\begin{aligned}
p_\varphi(\varphi) =& \frac{\gamma}{2\alpha^2(\varphi)} + \frac{\gamma\beta(\varphi)\sqrt{\pi}}{4\alpha^3(\varphi)}\mathrm{e}^{\frac{\beta^2(\varphi)}{4\alpha^2(\varphi)}} \\
&\cdot \left[1 + \mathrm{erf}\left(\frac{\beta(\varphi)}{2\alpha(\varphi)}\right)\right].
\end{aligned} \tag{31}$$

The probability density of the estimated frequency deviation

$$\hat{f}_\mathrm{d} = \frac{\arg(\Psi)}{2\pi T_\mathrm{i}} = \frac{\arg\left(\sum_{\mu=1}^{M} s_\mu s_{\mu-1}^*\right)}{2\pi T_\mathrm{i}} = \frac{\varphi}{2\pi T_\mathrm{i}} \tag{32}$$

$$\hat{f}_\mathrm{d} \in \left[-\frac{1}{2T_\mathrm{i}}, \frac{1}{2T_\mathrm{i}}\right] \tag{33}$$

is therefore

$$p_{\hat{f}_\mathrm{d}}(\hat{f}_\mathrm{d}) = \frac{2\pi T_\mathrm{i}\gamma}{2\tilde{\alpha}^2(\hat{f}_\mathrm{d})} + \frac{2\pi T_\mathrm{i}\gamma\tilde{\beta}(\hat{f}_\mathrm{d})\sqrt{\pi}}{4\tilde{\alpha}^3(\hat{f}_\mathrm{d})} \mathrm{e}^{\frac{\tilde{\beta}^2(f_\mathrm{d})}{4\tilde{\alpha}^2(f_\mathrm{d})}} \cdot \left[1 + \mathrm{erf}\left(\frac{\tilde{\beta}(\hat{\mathrm{f}}_\mathrm{d})}{2\tilde{\alpha}(\hat{\mathrm{f}}_\mathrm{d})}\right)\right], \tag{34}$$

$$\tilde{\alpha}(\hat{f}_\mathrm{d}) \triangleq \sqrt{\frac{\cos^2(2\pi T_\mathrm{i}\hat{f}_\mathrm{d})}{2\sigma_x^2} + \frac{\sin^2(2\pi T_\mathrm{i}\hat{f}_\mathrm{d})}{2\sigma_y^2}}, \tag{35}$$

$$\tilde{\beta}(\hat{f}_\mathrm{d}) \triangleq \frac{m_x\cos(2\pi T_\mathrm{i}\hat{f}_\mathrm{d})}{\sigma_x^2} + \frac{m_y\sin(2\pi T_\mathrm{i}\hat{f}_\mathrm{d})}{\sigma_y^2}. \tag{36}$$

6. ESTIMATION PERFORMANCE

Fig. 3 shows the expectation value of the estimated frequency deviation $\hat{f}_\mathrm{d}$

$$m_{\hat{f}_\mathrm{d}} = \mathrm{E}\{\hat{f}_\mathrm{d}\} = \frac{\int_{-\pi}^{\pi}\varphi\, p_\varphi(\varphi)\, d\varphi}{2\pi T_\mathrm{i}} \tag{37}$$

and its standard deviation

$$\sigma_{\hat{f}_\mathrm{d}} = \sqrt{\mathrm{E}\left\{\left(\hat{f}_\mathrm{d} - \mathrm{E}\{\hat{f}_\mathrm{d}\}\right)^2\right\}} = \frac{\sqrt{\int_{-\pi}^{\pi}(\varphi - \mathrm{E}\{\varphi\})^2\, p_\varphi(\varphi)\, d\varphi}}{2\pi T_\mathrm{i}} \tag{38}$$

versus the total observation time

$$T_\mathrm{o} = N(M+1)T_\mathrm{s} \tag{39}$$

for different actual frequency deviations f_d and different signal-to-noise ratios (SNR). It can be seen from Fig.3 that the presented frequency offset estimation method performs well at very low SNR values. This is important because these low SNR values are commonly found in enhanced sensitivity Galileo/GPS applications with operations in moderate indoor and dense urban environments.

The method, furthermore, converges relatively fast towards the actual frequency deviation f_d, when compared to typical dwell times for enhanced sensitivity Galileo/GPS receivers, which are in the order of several hundred milliseconds. The reason for the initial bias for short observation periods and low SNR values can be illustrated with (17) and (18). Since the variance of the real part and the variance of the imaginary part of the random variable Ψ are different, estimating the phase of Ψ generally leads to a bias. This bias, however, becomes much smaller when the SNR value of the received signal improves and when the observation time increases, since longer noncoherent integration numbers M lead to a larger SNR value of Ψ.

The presented estimation method also provides a sufficiently low standard deviation, such that the remaining frequency error $\hat{f}_\mathrm{d}$ has no significant impact on the reception sensitivity, since the term $\mathrm{sinc}^2(\hat{f}_\mathrm{d}T_\mathrm{i})$ in (15) and (16) delivers values larger than 0.999.

7. CONCLUSION

Estimating the residual frequency deviation can substantially improve the reception sensitivity of Galileo/GPS receivers and is therefore particularly important for urban and moderate indoor applications, where the weak Galileo/GPS signals are further attenuated. The presented frequency offset estimation method integrates very well with Galileo/GPS receivers based on differential correlation, where most of the existing signal processing steps can be reused and only minimal additional signal processing is required. It has no problems with phase jumps and performs well for the very low signal to noise ratios, which are frequently encountered for urban and moderate indoor Galileo/GPS reception.

8. REFERENCES

[1] P. Ciblat and L. Vandendrope, "Blind carrier frequency estimation for noncircular constellation-based transmissions," *IEEE Transactions on Signal Processing*, vol. 51, no. 5, pp. 1378-1389, May 2003.

[2] E. Serpedin, A. Chevreuil, G.B. Giannakis, and P. Laubaton, "Blind channel and carrier frequency offset estimation using periodic modulation precoders," *IEEE Transactions on Signal Processing*, vol. 48, no. 8, pp. 2389-2405, August 2000.

[3] U. Tureli, P.J. Honan, and H. Liu, "Low-complexity nonlinear least squares carrier offset estimator for OFDM: identifiability, diversity, and performance," *IEEE Transactions on Signal Processing*, vol. 52, no. 9, pp. 2441-2452, Sept. 2004.

[4] Y. Wang, E. Serpedin, and P. Ciblat, "Optimal blind nonlinear least-square carrier phase and frequency offset estimation for general QAM modulations," *IEEE Transactions on Wireless Communications*, vol. 2, no. 5, pp. 1040-1054, Sept. 2003.

[5] A. Schmid and A. Neubauer, "Comparison of the sensitivity limits for GPS and Galileo receivers in multipath scenarios," *Proc. IEEE Position Location and Navigation*, pp. 503-509, April 2004.

[6] A. Schmid and A. Neubauer, "Differential correlation for Galileo/GPS receivers," *Proc. IEEE Int. Conference on Acoustics, Speech, and Signal Processing*, vol. 3, pp. 953-956, March 2005.

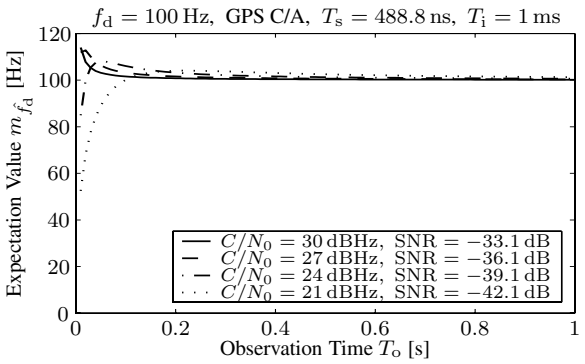

(a) Expectation value $m_{\hat{f}_\mathrm{d}}$ for $f_\mathrm{d} = 100$ Hz

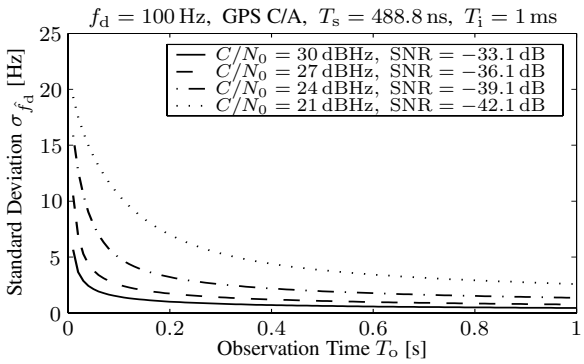

(b) Standard deviation $\sigma_{\hat{f}_\mathrm{d}}$ for $f_\mathrm{d} = 100$ Hz

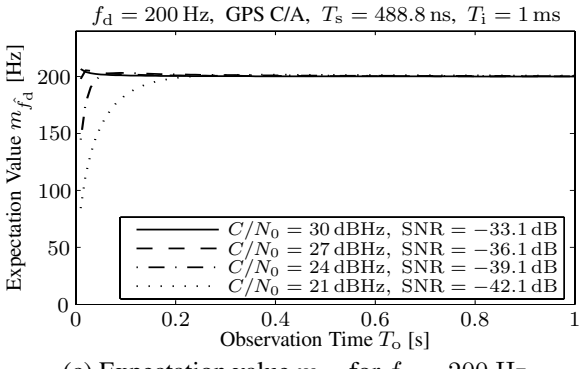

(c) Expectation value $m_{\hat{f}_\mathrm{d}}$ for $f_\mathrm{d} = 200$ Hz

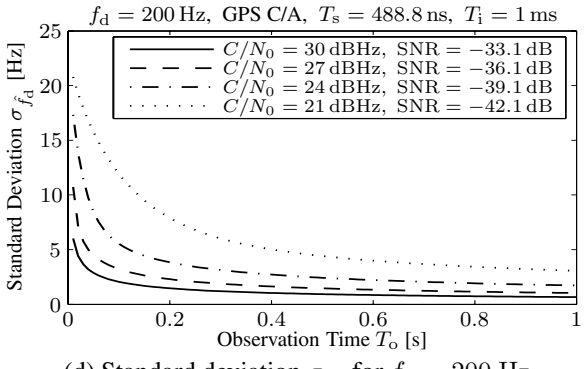

(d) Standard deviation $\sigma_{\hat{f}_\mathrm{d}}$ for $f_\mathrm{d} = 200$ Hz

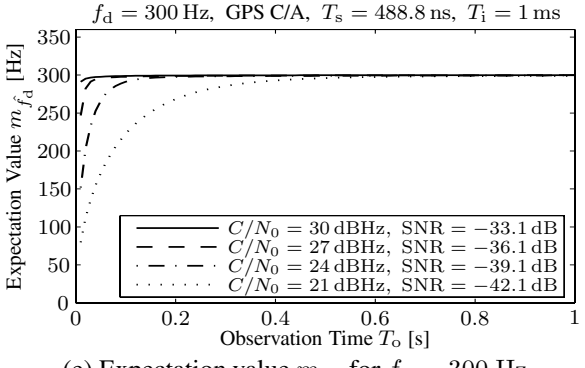

(e) Expectation value $m_{\hat{f}_\mathrm{d}}$ for $f_\mathrm{d} = 300$ Hz

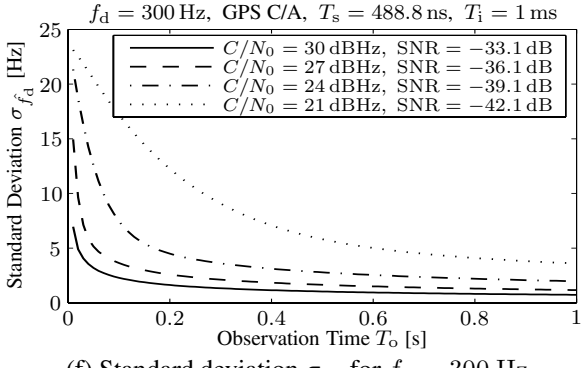

(f) Standard deviation $\sigma_{\hat{f}_\mathrm{d}}$ for $f_\mathrm{d} = 300$ Hz

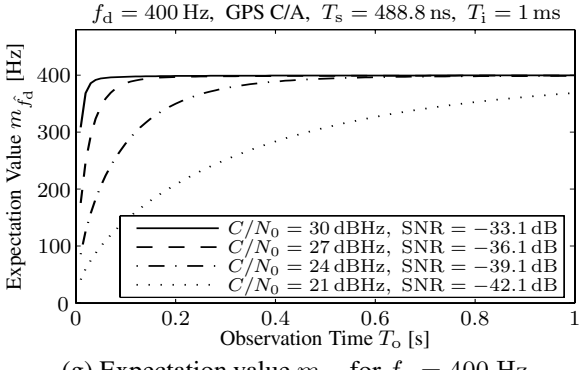

(g) Expectation value $m_{\hat{f}_\mathrm{d}}$ for $f_\mathrm{d} = 400$ Hz

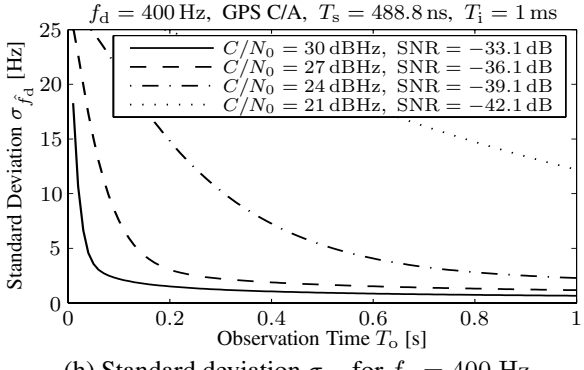

(h) Standard deviation $\sigma_{\hat{f}_\mathrm{d}}$ for $f_\mathrm{d} = 400$ Hz

Fig. 3. Performance of the frequency offset estimation.